

The N-terminus of hepcidin is essential for its interaction with ferroportin: structure-function study

Elizabeta Nemeth, Gloria C. Preza, Chun-Ling Jung, Jerry Kaplan, Alan J. Waring, and Tomas Ganz

Hepcidin is the principal iron-regulatory hormone. It acts by binding to the iron exporter ferroportin, inducing its internalization and degradation, thereby blocking cellular iron efflux. The bioactive 25 amino acid (aa) peptide has a hairpin structure stabilized by 4 disulfide bonds. We synthesized a series of hepcidin derivatives and determined their bioactivity in a cell line expressing ferroportin-GFP fusion protein, by measuring the degradation of ferroportin-GFP and the accumulation of ferritin after peptide treatment. Bioactiv-

ity was also assayed in mice by the induction of hypoferremia. Serial deletion of N-terminal amino acids caused progressive decrease in activity which was completely lost when 5 N-terminal aa's were deleted. Synthetic 3-aa and 6-aa N-terminal peptides alone, however, did not internalize ferroportin and did not interfere with ferroportin internalization by native hepcidin. Deletion of 2 C-terminal aa's did not affect peptide activity. Removal of individual disulfide bonds by pairwise substitution of cysteines with alanines also did not

affect peptide activity in vitro. However, these peptides were less active in vivo, likely because of their decreased stability in circulation. G71D and K83R, substitutions previously described in humans, did not affect hepcidin activity. Apart from the essential nature of the N-terminus, hepcidin structure appears permissive for mutations. (Blood. 2006;107:328-333)

© 2006 by The American Society of Hematology

Introduction

Hepcidin, a peptide hormone produced by the liver, is the principal regulator of iron homeostasis. Hepcidin production increases with iron loading and inflammation and decreases with anemia and hypoxia.^{1,2} Hepcidin acts by binding to ferroportin, the sole cellular iron exporter, and inducing its internalization and degradation.³ Because ferroportin is expressed in the duodenum, spleen, liver, and placenta,⁴ hepcidin increase, and the subsequent decrease of ferroportin, results in inhibition of duodenal iron absorption, release of recycled iron from macrophages, mobilization of iron stores from the liver, and iron transfer across placenta. Excessive hepcidin production resulting from increased expression in liver tumors⁵ or transgene expression,⁶ or acute administration of synthetic hepcidin,⁷ leads to either acute or chronic hypoferremia. Alternatively, hepcidin deficiency resulting from mutations in the hepcidin gene itself, or the genes encoding HFE, transferrin receptor 2, or hemojuvelin,⁸⁻¹¹ appears to be the cause of most types of hereditary hemochromatosis.

The hepcidin gene encodes an 84-amino acid prepropeptide with a typical signal sequence and a consensus cleavage site for a prohormone convertase that generates the mature bioactive 25-amino acid form found in plasma and urine.^{12,13} The 25-amino acid peptide (hep25) forms a hairpin loop stabilized by 4 disulfide

bonds, one of which is an unusual vicinal bond between adjacent cysteines at the hairpin turn.¹⁴ Three-dimensional nuclear magnetic resonance (3D-NMR) structure studies also showed that hepcidin is an amphipathic peptide similar to most antimicrobial peptides. However, unlike antimicrobial peptides that display great species-to-species variation, hepcidin sequence is conserved across species, ranging from fish to mammals, with human sequence showing 60% similarity to the zebra fish hepcidin-1.¹⁵

Here, we report on an investigation of hepcidin structure in relation to its function and show that the N-terminus of hepcidin is critical for its iron-regulatory activity.

Materials and methods

Peptide synthesis

The peptides were synthesized on an ABI 431A peptide synthesizer (PE Biosystems, Applied Biosystems, Foster City, CA) using fmoc amino acids, Wang resin (AnaSpec, San Jose, CA), and double coupling for all residues. After cleavage, 30 mg crude peptides was reduced with 1000-fold molar excess of dithiothreitol (DTT) in 0.5 M Tris buffer (pH 8.2), 6 M guanidine hydrochloride, and 20 mM EDTA at 52°C for 2 hours. Fresh DTT

From the Department of Medicine, David Geffen School of Medicine, Los Angeles, CA; the Department of Pathology, David Geffen School of Medicine, Los Angeles, CA; and the Department of Pathology, School of Medicine, University of Utah, Salt Lake City, UT.

Submitted May 23, 2005; accepted August 22, 2005. Prepublished online as *Blood* First Edition Paper, September 1, 2005; DOI 10.1182/blood-2005-05-2049.

Supported by the National Institutes of Health (grants R37 DK030534 and R01 DK070947-0)1 (J.K.), (grant DK 065029) (T.G.), and by the Will Rogers Fund (T.G.).

E.N. planned and designed the studies, performed or supervised most of the experiments, evaluated the experiments, and cowrote the manuscript. G.C.P. and C.-L.J. performed peptide purification and refolding and FACS analysis and analyzed the data. J.K. planned the studies, participated in the

development of the methodology, and cowrote the manuscript. A.J.W. planned and performed peptide syntheses, participated in peptide design, analyzed peptide conformations, and cowrote the manuscript. T.G. planned the studies and experiments, supervised and helped evaluate them, participated in peptide design, and cowrote the manuscript.

The online version of this article contains a data supplement.

Reprints: Tomas Ganz, 37-055 CHS, Department of Medicine, David Geffen School of Medicine at UCLA, Los Angeles, CA 90095-1690; e-mail: tganz@mednet.ucla.edu

The publication costs of this article were defrayed in part by page charge payment. Therefore, and solely to indicate this fact, this article is hereby marked "advertisement" in accordance with 18 U.S.C. section 1734.

© 2006 by The American Society of Hematology

(500-molar excess) was added and incubated for an additional hour at 52°C. The reduced peptides were purified on the 10-g C18 Sep-Pak cartridges (Waters, Milford, MA) equilibrated in 0.1% TFA and eluted with 50% acetonitrile. The eluates were lyophilized and resuspended in 0.1% acetic acid. The reduced peptides were further purified by reversed-phase high-performance liquid chromatography (RP-HPLC) on Vydac C18 column (218TP510; Waters) equilibrated with 0.1% trifluoroacetic acid and eluted with an acetonitrile gradient. The eluates were lyophilized, dissolved in 0.1% acetic acid, 20% DMSO, to the approximate concentration of 0.1 mg/mL (pH 8), and air oxidized by stirring for 18 hours at room temperature. The refolded peptides were also purified sequentially on the 10-g C18 Sep-Pak cartridge and on the RP-HPLC Vydac C18 column using an acetonitrile gradient. The eluates were lyophilized and resuspended in 0.016% HCl. The conformation of refolded synthetic hepcidin derivatives was verified by electrophoresis in 12.5% acid-urea polyacrylamide gel electrophoresis (PAGE), and peptide masses were determined by matrix-assisted laser desorption/ionization time-of-flight mass spectrometry (MALDI-TOF-MS; UCLA Mass Spectrometry Facility, Los Angeles, CA). Of note, the C11A/C19A peptide was modified at the C-terminus by tert-butyl because of incomplete removal of the protective group following the crude peptide synthesis. All of the other peptides had masses that matched predictions.

Circular dichroism spectroscopy

Circular dichroism spectra (185–260 nm) of the hepcidin peptides were recorded on an AVIV 62DS spectropolarimeter (AVIV Associates, Lakewood, NJ). The instrument was calibrated for wavelength and optical rotation using d-10-camphorsulphonic acid.¹⁶ Samples were scanned at a temperature of 25°C using 0.01-cm path length cells at a rate of 10 nm per minute and a sample interval of 0.2 nm. Sample concentration was determined by quantitative amino acid analysis (UC Davis Core Facility, Davis, CA), and the sample concentration of the peptides was 200 μM in a solution containing 25 mM HEPES buffer, pH 7.5 with 150 mM NaCl. Before analysis, spectra were baseline corrected by subtracting spectra of peptide-free buffer solution from the peptide-containing sample and expressed as the Mean Residue Ellipticity θ_{MRE} . Quantitative estimates of the secondary structural contributions were made with SELCON 3¹⁷ using spectral basis set 8 for soluble proteins implemented in the Olis Global Works software package (Olis, Bogart, GA).

Flow cytometry

ECR293-Fpn, a cell line stably transfected with the mouse ferroportin-GFP construct under the control of ponasterone-inducible promoter, was prepared and maintained as previously described.³ The cells were plated on poly-D-lysine-coated plates in the presence of 20 μM FAC, with or without 10 μM ponasterone. After 24 hours, ponasterone was washed off, and cells were treated with peptides for 24 hours. Cells were then trypsinized and resuspended at 1×10^6 cells/mL, and the intensity of green fluorescence was analyzed by flow cytometry at the UCLA Jonsson Comprehensive Cancer Center and Center for AIDS Research Flow Cytometry Core Facility (supported by NIH awards CA-16 042 and AI-28 697, Jonsson Cancer Center, the UCLA AIDS Institute, and the UCLA School of Medicine). Flow cytometry was performed on FACScan (fluorescence activated cell scanner) Analytic Flow Cytometer (Becton Dickinson, San Jose, CA) with CellQuest version 3.3 software (Becton Dickinson). Cells not induced with ponasterone to express Fpn-GFP were used to establish a gate to exclude background fluorescence. Cells induced with ponasterone, but not treated with any peptides, were used as the positive control. Each peptide treatment was repeated independently 3 to 6 times. The results were expressed as a fraction of the activity of hep25, according to the formula $1 - [(F_x - F_{hep25}) / (F_{untreated} - F_{hep25})]$, where F was the mean of the gated green fluorescence and x was the peptide.

Ferritin measurements

ECR293-Fpn cells were incubated with 20 μM FAC with or without 10 μM ponasterone. After 24 hours, ponasterone was washed off, and hepcidin

derivatives were added for 24 hours in the presence of 20 μM FAC. Cellular protein was extracted with 150 mM NaCl, 10 mM EDTA, 10 mM Tris (pH 7.4), 1% Triton X-100, and a protease inhibitor cocktail (Sigma-Aldrich, St Louis, MO). Ferritin levels were determined by an enzyme-linked immunosorbent assay (ELISA) assay (Ramco Laboratories, Stafford, TX, or Biotech Diagnostic, Laguna Niguel, CA) according to the manufacturer's instructions and were normalized for the total protein concentration in each sample, as determined by the bicinchoninic acid (BCA) assay (Pierce, Rockford, IL). The results were expressed as the relative change in ferritin, according to the formula $(F_x - F_{untreated}) / (F_{hep25} - F_{untreated})$, where F was the ferritin concentration (ng/mg protein) and x was the peptide.

Mouse serum iron measurements

Animal studies were approved by the Animal Research Committee at UCLA. C57BL/6 mice were obtained from The Jackson Laboratory (Bar Harbor, ME) and were maintained on NIH 31 rodent diet (iron content 336 mg/kg; Harlan Teklad, Indianapolis, IA). Two weeks before the experiment, the mice were switched to an iron-deficient diet containing 2 to 4 ppm iron (Harlan Teklad) to suppress endogenous hepcidin. Mice were injected intraperitoneally either with 100 μL PBS (control) or with 50 μg peptide in 100 μL PBS. Mice were killed 2 hours later, blood was collected by cardiac puncture, and serum was separated using Microtainer tubes (Becton Dickinson, Franklin Lakes, NJ). Serum iron was determined by using a colorimetric assay (Diagnostic Chemicals, Oxford, CT), which was modified for the microplate format¹⁸ so that 50 μL serum was used per measurement. The results were expressed as the percentage of decrease in serum iron when compared with the average value of serum iron levels in PBS-injected mice.

Statistics

We used Sigma Stat version 3.0 for statistical analyses (Systat Software, Point Richmond, CA).

Results

We synthesized a series of hepcidin peptides with alterations targeting the N-terminus, C-terminus, and the disulfide bonding pattern, or with substitutions found in patients with iron overload (Figure 1). After the peptides were folded and purified, their structure was analyzed by circular dichroism (CD) spectroscopy. All spectra were typical of disulfide-stabilized β sheet peptides connected by turn-loop segments.^{13,19,20} Analysis of the CD spectra indicated that the general conformational characteristics were preserved in all the structures (Table 1). Even CD spectra of disulfide-modified hepcidins (Figure 2), including the shortened peptide lacking 3 of the 4 disulfide bonds, indicated little effect on conformation.

We next analyzed the effect of structural alterations on the peptide bioactivity. We previously used a cell line (ECR293) stably transfected with the mouse ferroportin-GFP fusion protein³ to show that hepcidin causes internalization and degradation of iron export channel ferroportin. In this study, we used the same ECR293 in vitro model but accurately measured the degradation of ferroportin-GFP by flow cytometry after treatment with different peptides (Supplemental Figure S1, available at the *Blood* website; see the Supplemental Figure link at the top of the online article). Table 2 shows a summary of the peptide activities and their statistical analysis. The serial deletion of the N-terminal amino acids caused a progressive loss of activity, with almost complete loss when all 5 residues were deleted (del1-5(DTHFP), also known as hep20) (Figure 3A). To determine whether the N-terminus by itself could serve as hepcidin agonist or antagonist, we synthesized the 3-amino acid (DTH) and 6-amino acid (DTHFPI) N-terminal peptides. The

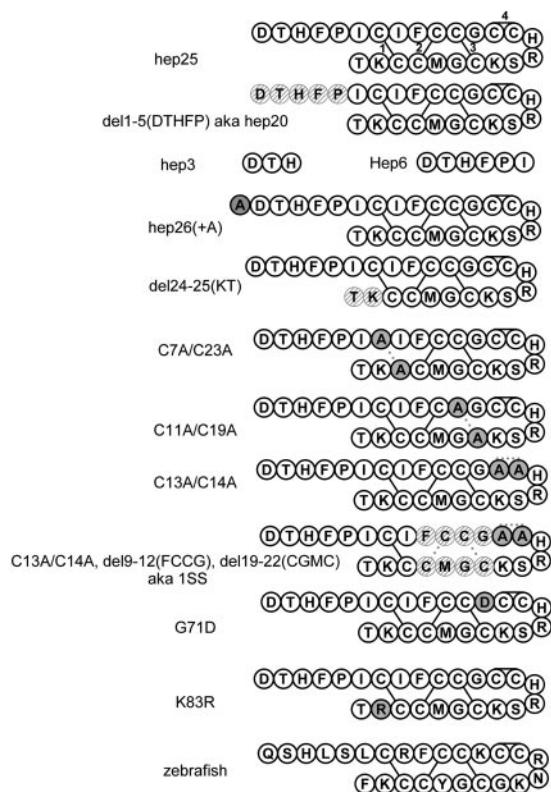


Figure 1. Schematic representation of hepcidin derivatives. Hatched circles represent deleted residues. Solid light gray circles represent substitutions. The numbering system refers to hep25, so that residues 1 to 25 correspond to residues 60 to 84 of the prepropeptide. In conformity with the original reports of these mutations, G71D and K83R refer to the prepropeptide numbering system.

peptides did not internalize ferroportin and, even at 20-fold higher concentrations, did not interfere with ferroportin degradation induced by hep25 (Table 2). The N-truncated inactive peptide Hep20 (5 μ M) also did not interfere with the full-length peptide (1 μ M) when the 2 were simultaneously added to the cells (Table 2).

The peptide extended at the N-terminus by the addition of Ala (hep26(+A)) had activity equivalent to hep25 (Figure 3A). When amino acid residues from the C-terminus were deleted (del24-25(KT)), the peptide activity was only slightly affected ($90\% \pm 7\%$; Figure 3A).

We also altered the disulfide-bonding pattern by replacing pairs of cysteines with alanines so that C7A/C23A derivative lacked the most terminal disulfide bond (bond 1), C11A/C19A lacked bond 3, and C13A/C14A lacked the vicinal bond (bond 4). The 3 peptides exhibited nearly full activity ($85\% \pm 3\%$, $92\% \pm 6\%$, $92\% \pm 12\%$, mean \pm SD, respectively; Figure 3A). CD spectroscopy indicated

Table 1. Secondary structures of hepcidin variants

Sample*	β sheet, %	Turn, %	Disordered, %
hep25	30.0	28.0	42.0
hep20	32.0	29.0	39.0
delKT	30.0	30.0	40.0
K83R	29.0	27.0	44.0
G71D	29.0	29.0	42.0
1SS	31.0	25.0	44.0
C7A/C23A	26.0	26.0	48.0
C11A/C19A	25.0	26.0	49.0
C13A/C14A	30.0	26.0	44.0

*The percentage of helix for all samples was 0.

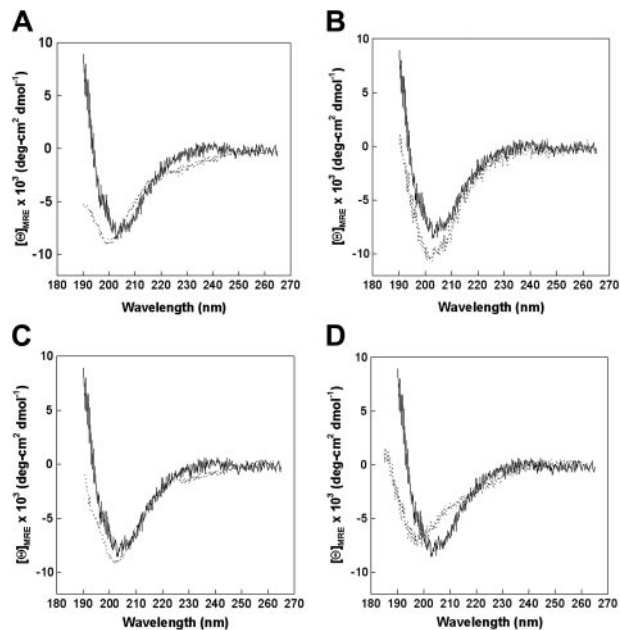


Figure 2. Representative CD spectra of parent hep25 peptide and disulfide bond variants. Hep25 (solid lines) was compared to hepcidin C13A/C14A (A), hepcidin C7A/C23A (B), hepcidin C11A/C19A (C), and hepcidin 1SS (del9-12 [FCCG], del19-22 [CGMC], C13A/C14A) (D).

that these substitutions did not significantly change the molecule's hairpin structure (Figure 2). The peptide with a significantly shortened hairpin and lacking 3 of 4 disulfide bonds (del9-12(FCCG), del19-22(CGMC), C13A/C14A; abbreviated as 1SS) still showed $54\% \pm 5\%$ activity.

Table 2. Summary of hepcidin derivative bioactivity

Peptide	Flow cytometry		Ferritin ELISA	
	Hepcidin-25 activity, %	P	Hepcidin-25 activity, %	P
Hep24	95 \pm 4	.018	77 \pm 19	.034
Hep23	88 \pm 4	< .001	47 \pm 28	.003
Hep22	46 \pm 6	< .001	13 \pm 16	< .001
Hep21	22 \pm 3	< .001	3 \pm 6	< .001
Hep20	12 \pm 8	< .001	3 \pm 6	< .001
Hep3	-6 \pm 10	< .001	-2 \pm 10	< .001
Hep6	1 \pm 3	< .001	-5 \pm 5	< .001
Hep26	100 \pm 1	NS	—	—
delKT	90 \pm 7	.01	87 \pm 18	NS
C7A/C23A	85 \pm 3	< .001	107 \pm 12	NS
C11A/C19A	92 \pm 6	.014	101 \pm 9	NS
C13A/C14A	92 \pm 12	NS	84 \pm 21	NS
1SS	54 \pm 5	< .001	36 \pm 29	< .001
G71D	108 \pm 1	< .001	91 \pm 11	NS
K83R	101 \pm 3	NS	107 \pm 17	NS
zebrafish	106 \pm 10	NS	103 \pm 8	NS
hep25 + 20; 5 μ M	102 \pm 2	.05	—	—
hep3; 20 μ M	-10 \pm 7	< .001	—	—
hep25 + 3; 20 μ M	102 \pm 3	NS	—	—
hep6; 20 μ M	6 \pm 4	< .001	—	—
hep25 + 6; 20 μ M	96 \pm 4	.047	—	—

The results, expressed as percentage of the hep25 activity, are the mean \pm SD of 3 to 6 independent experiments. The values obtained by flow cytometry represent the ability of peptide to cause degradation of ferroportin-GFP, and the values obtained by ferritin ELISA represent the peptides' ability to cause cellular iron retention. Each peptide was added at the concentration of 1 μ M, unless indicated otherwise. Paired *t* test was used for statistical analysis for each peptide in comparison to hep25.

NS indicates not significant (> .05); —, not done.

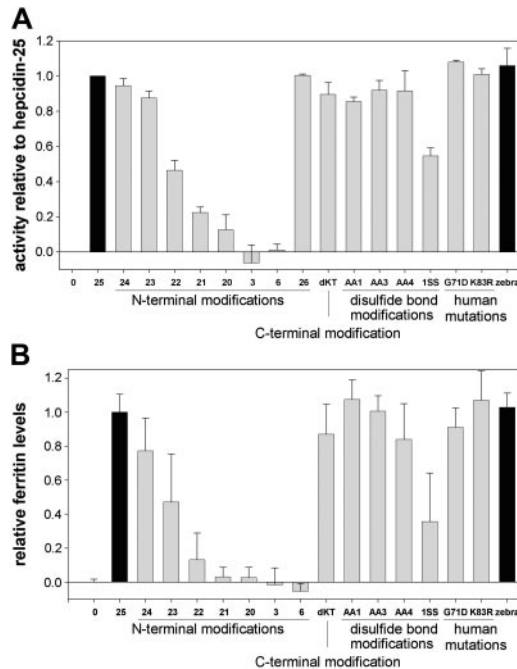


Figure 3. Relative activity of hepcidin derivatives. (A) Flow cytometry measuring degradation of ferroportin-GFP. (B) Ferritin ELISA measuring cellular iron retention. For both panels, the values were expressed as a fraction of hep25 activity. Peptides were added to cells for 24 hours at $1 \mu\text{M}$ concentration, except for hep3 and hep6, which were added at $4 \mu\text{M}$. 25 = hep25; 24 to 20 = del1-5(DTHFP); 3 = hep3 (DTH); 6 = hep6 (DTHFP1); 26 = hep26(+A); dKT = del24-25(KT); AA1 = C7A/C13A; AA3 = C11A/C19A; AA4 = C13A/C14A; 1SS = [del9-12(FCCG), del19-22(CGMC), C13A/C14A]; zebra = zebra fish. The activities corresponding to the unmodified, naturally occurring active forms of hepcidin are shown as black bars.

We also synthesized peptides with substitutions found in patients with iron overload disorders. Heterozygous G71D substitution was described in patients with HFE-related hemochromatosis,²¹⁻²³ and heterozygous K83R substitution was found in a patient with porphyria cutanea tarda and iron overload (J.K. and John Phillips, University of Utah; unpublished observations, December 2004). G71D and K83R peptides, however, had activity similar to wild-type hep25 (Figure 3A).

Zebra fish hepcidin-1, which has only 52% identity with human hepcidin but preserves the disulfide structure and the general amphipathic character of the molecule, also caused ferroportin degradation comparable to human hep25.

Hepcidin-induced ferroportin internalization and degradation cause cellular iron retention.³ We measured accumulation of the iron storage protein ferritin after treatment with hepcidin derivatives as an additional assessment of peptide bioactivity. The activity of peptides as determined by ferritin ELISA paralleled the results obtained from flow cytometry (Figure 3B; Table 2). N-terminus deletion resulted in the loss of activity, C-terminus deletion (delKT), or disulfide bonds replacements (C7A/C23A, C11A/C19A, and C13A/C14A) showed nearly full activity ($87\% \pm 18\%$, $107\% \pm 12\%$, $100\% \pm 9\%$, and $84\% \pm 21\%$, mean \pm SD, respectively), while the short hairpin lacking 3 disulfide bonds (1SS) had $36\% \pm 29\%$ activity when compared with hep25. The N-terminal 3-aa or 6-aa peptides failed to cause ferritin accumulation, whereas zebra fish hepcidin-1 was fully active ($103\% \pm 8\%$ of the human hep25 activity).

Injection of synthetic human hep25 causes rapid hypoferrremia in mice.²⁴ We therefore measured serum iron in mice 2 hours after the injection of $50 \mu\text{g}$ selected hepcidin derivatives (Figure 4). Hep25, G71D, and K83R peptides caused a similar and significant

drop in serum iron compared with control mice injected with diluent. C13A/C14A peptide lacking the vicinal disulfide bond and delKT lacking the 2 C-terminal amino acids also significantly suppressed serum iron. Serum iron levels did not change significantly in mice injected with hep20, the short hairpin lacking 3 disulfide bonds (1SS), or the 2 peptides lacking disulfide bonds across the hairpin (C7A/C23A, C11A/C19A).

Discussion

Hepcidin regulates extracellular and plasma iron by controlling iron flows from the duodenum, macrophages, and liver.²⁵ This is achieved by hepcidin binding to the cellular iron exporter ferroportin and causing its internalization and degradation. Bioactive hepcidin is a 25-amino acid peptide; a simple hairpin stabilized by 4 disulfide bonds, one of which is an unusual vicinal bond.^{13,26} Hepcidin structure is conserved across species from fish to mammals, but some species (mouse, zebra fish) contain an additional hepcidin gene of unknown functional significance. Zebra fish hepcidin-1 shows only 52% identity with human hepcidin, but all 8 cysteines are in the same position as in human hepcidin. The substitutions in the important N-terminal are conservative, as indicated by similarity matrices derived from analyses of amino acid substitutions in evolutionarily-related proteins. For example, in the BLOSUM80 matrix,²⁷ the first 4 amino acids in the zebra fish sequence QSHL represent respectively the second, second, first, and third most conservative substitution for the amino acids of the human sequence DTHF. In our study, synthetic zebra fish hepcidin-1 was equivalent to human hepcidin in its ability to induce degradation of mouse ferroportin-GFP and cause cellular iron retention.

We next introduced a series of structural alterations into human hep25 to assess the functional importance of the N-terminal and C-terminal amino acids, as well as the disulfide-bonding pattern. The peptide bioactivity was assessed by quantitating ferroportin-GFP degradation and by measuring ferritin accumulation as an indicator of the inhibition of iron efflux. Some peptides were also tested for their ability to cause hypoferrremia in mice. Surprisingly, hepcidin structure was quite permissive to changes. The only major effect on activity was seen when the 5 N-terminal amino acids were serially deleted, resulting in a gradual loss of activity, with hep20

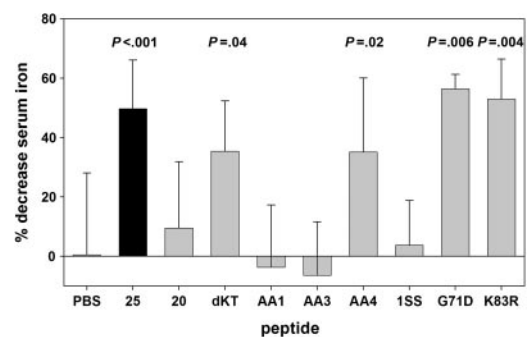


Figure 4. Activity of hepcidin derivatives in vivo. Diluent or peptides ($50 \mu\text{g}/\text{mouse}$) were injected in mice, and serum iron levels were determined after 2 hours. *P* values (Student *t* test) above bars denote statistically significant difference in comparison to PBS-injected mice. 25 = hep25; 20 = hep20 [del1-5(DTHFP)]; dKT = del24-25(KT); AA1 = C7A/C13A; AA3 = C11A/C19A; AA4 = C13A/C14A; 1SS = [del9-12(FCCG), del19-22(CGMC), C13A/C14A]. The activity corresponding to the naturally occurring active form of hepcidin is shown as a black bar. PBS and hep25 were each tested in 10 mice, and 4 to 6 mice were used for each of the other peptides.

showing an almost complete loss of the activity both in vitro and when injected in mice. Addition of 1 amino acid to the N-terminus, however, had no effect on the peptide's ability to induce ferroportin degradation. Deletion of 2 C-terminal amino acids also had no significant functional consequences.

Considering the essential nature of the N-terminus, we synthesized the 3- and 6-amino acid N-terminal peptides to assess their potential use as agonists or antagonists. The 2 peptides, however, did not mimic or interfere with the activity of hep25. The only other inactive peptide, N-terminally truncated hep20, also did not interfere with ferroportin degradation induced by full-length hep25.

Of interest, pairwise replacement of cysteines with alanines, which removed disulfide bonds 1, 3, or 4 one at a time, did not cause major changes in the peptide structure when analyzed by circular dichroism spectroscopy. Accordingly, the peptide bioactivity in vitro was not significantly affected. However, in mice, the 2 peptides lacking disulfide bonds across the hairpin (C7A/C23A, C11A/C19A) were inactive at the given dose, whereas C13A/C14A peptide lacking the vicinal disulfide bond was somewhat less effective than wild-type hep25. The high degree of disulfide bonding in small peptides likely confers greater stability and resistance to proteolytic degradation,²⁸ and peptides made to lack one or more disulfide bonds may have a shorter half-life in circulation.

We generated a shortened hairpin peptide with only one disulfide bond, by removing 8 residues [del19-12(FCCG), del19-22(CGMC)] in addition to replacing vicinal cysteines with alanines. Despite the significant structural alteration, the peptide still exhibited 50% activity in vitro. In vivo, however, injection of the single dose of shortened peptide in mice failed to cause a significant change in serum iron. The discrepancy between in vitro and in vivo activity is consistent with our expectations of decreased stability and shortened half-life of the mutant peptide.

Substitutions affecting cysteine residues that form disulfide bonds in the mature hepcidin have been identified in patients with juvenile hemochromatosis (C70R and C78T, both affecting bond 3)²⁹ and in a patient with adult hemochromatosis (compound heterozygous hepcidin mutations R59G and C82Y, the latter affecting bond 1).³⁰ The substitution of a single cysteine residue, however, would lead to the appearance of an unpaired cysteine and would likely initiate the formation of incorrect disulfide bonds and degradation of the aberrant peptides inside the cell,^{31,32} resulting in

reduced production of the bioactive peptide. Hepcidin concentrations in these patients, however, have not yet been assessed.

Hepcidin disease-causing mutations described so far²⁹ include the previously mentioned substitutions of single cysteines, as well as the premature stop codon, out-of-frame start codon, and frameshift, all expected to produce no mature peptide. The only other missense mutations in the region coding for mature peptide were generally found in the heterozygous state and have an as yet uncertain phenotypic effect. G71D was found as a possible modifier in patients with hemochromatosis carrying HFE C282Y mutations,²¹⁻²³ and K83R was found in a patient with porphyria cutanea tarda and iron overload (J.K. and John Phillips, University of Utah; unpublished observations, December 2004). Synthetic G71D and K83R peptides were fully functional in in vitro assays as well as in the mouse hypoferremia assay. These findings would suggest that neither of these hepcidin mutations is likely to be important modifiers in iron overload diseases.

It may appear counterintuitive that the hepcidin-ferroportin interaction is so tolerant of hepcidin mutations. However, the estimated affinity of the hepcidin-ferroportin interaction is relatively low both in vitro and in vivo (~ 500 nM),^{3,33} so a maximal molecular fit between the 2 structures is not necessary. In vivo, the low affinity of the hepcidin-ferroportin interaction would require large concentration of hepcidin in the target tissues, achievable because of the very large size of the hepcidin-producing organ (the liver) and relatively high rates of hepcidin synthesis, at least as estimated from mRNA abundance in gene array experiments.³⁴

In conclusion, our study revealed the N-terminus of hepcidin is essential for its bioactivity, but the structure was otherwise surprisingly permissive for changes. Further studies of hepcidin structure in relation to its function are vital for the design of hepcidin antagonists and agonists, which could be used for treatment of iron disorders.

Acknowledgments

We thank Dr Seth Rivera and Victoria Gabayan for their help and advice with animal studies and Dr John Phillips from the University of Utah, Salt Lake City, for sharing with us his data on a patient with a hepcidin mutation.

References

- Pigeon C, Ilyin G, Courselaud B, et al. A new mouse liver-specific gene, encoding a protein homologous to human antimicrobial peptide hepcidin, is overexpressed during iron overload. *J Biol Chem*. 2001;276:7811-7819.
- Nicolas G, Chauvet C, Viatte L, et al. The gene encoding the iron regulatory peptide hepcidin is regulated by anemia, hypoxia, and inflammation. *J Clin Invest*. 2002;110:1037-1044.
- Nemeth E, Tuttle MS, Powelson J, et al. Hepcidin regulates cellular iron efflux by binding to ferroportin and inducing its internalization. *Science*. 2004;306:2090-2093.
- Donovan A, Lima CA, Pinkus JL, et al. The iron exporter ferroportin/Slc40a1 is essential for iron homeostasis. *Cell Metab*. 2005;1:191-200.
- Weinstein DA, Roy CN, Fleming MD, et al. Inappropriate expression of hepcidin is associated with iron refractory anemia: implications for the anemia of chronic disease. *Blood*. 2002;100:3776-3781.
- Nicolas G, Bennoun M, Porteu A, et al. Severe iron deficiency anemia in transgenic mice expressing liver hepcidin. *Proc Natl Acad Sci U S A*. 2002;99:4596-4601.
- Rivera S, Liu L, Nemeth E, et al. Hepcidin excess induces the sequestration of iron and exacerbates tumor-associated anemia. *Blood*. 2005;105:1797-1802.
- Roetto A, Papanikolaou G, Politou M, et al. Mutant antimicrobial peptide hepcidin is associated with severe juvenile hemochromatosis. *Nat Genet*. 2003;33:21-22.
- Bridle KR, Frazer DM, Wilkins SJ, et al. Disrupted hepcidin regulation in HFE-associated haemochromatosis and the liver as a regulator of body iron homeostasis. *Lancet*. 2003;361:669-673.
- Papanikolaou G, Samuels ME, Ludwig EH, et al. Mutations in HFE2 cause iron overload in chromosome 1q-linked juvenile hemochromatosis. *Nat Genet*. 2004;36:77-82.
- Nemeth E, Roetto A, Garozzo G, Ganz T, Camaschella C. Hepcidin is decreased in TFR2-hemochromatosis. *Blood*. 2004;105:1803-1806.
- Krause A, Neitz S, Magert HJ, et al. LEAP-1, a novel highly disulfide-bonded human peptide, exhibits antimicrobial activity. *FEBS Lett*. 2000;480:147-150.
- Park CH, Valore EV, Waring AJ, Ganz T. Hepcidin, a urinary antimicrobial peptide synthesized in the liver. *J Biol Chem*. 2001;276:7806-7810.
- Hunter HN, Fulton DB, Ganz T, Vogel HJ. The solution structure of human hepcidin, a peptide hormone with antimicrobial activity that is involved in iron uptake and hereditary hemochromatosis. *J Biol Chem*. 2002;277:37597-37603.
- Shike H, Shimizu C, Lauth X, Burns JC. Organization and expression analysis of the zebrafish hepcidin gene, an antimicrobial peptide gene conserved among vertebrates. *Dev Comp Immunol*. 2004;28:747-754.
- Miles AJ, Wien F, Lees JG, et al. Calibration and standardisation of synchrotron radiation circular dichroism and conventional circular dichroism spectrophotometers. *Spectroscopy*. 2003;17:653-661.

17. Sreerama N, Venyaminov SY, Woody RW. Estimation of the number of alpha-helical and beta-strand segments in proteins using circular dichroism spectroscopy. *Protein Sci.* 1999;8:370-380.
18. Nemeth E, Rivera S, Gabayan V, et al. IL-6 mediates hypoferrremia of inflammation by inducing the synthesis of the iron regulatory hormone hepcidin. *J Clin Invest.* 2004;113:1271-1276.
19. Tam JP, Lu YA, Yang JL. Design of salt-insensitive glycine-rich antimicrobial peptides with cyclic tricyclic structures. *Biochemistry.* 2000;39:7159-7169.
20. Cole AM, Hong T, Boo LM, et al. Retrocyclin: a primate peptide that protects cells from infection by T- and M-tropic strains of HIV-1. *Proc Natl Acad Sci U S A.* 2002;99:1813-1818.
21. Merryweather-Clarke AT, Cadet E, Bornford A, et al. Digenic inheritance of mutations in HAMP and HFE results in different types of haemochromatosis. *Hum Mol Genet.* 2003;12:2241-2247.
22. Jacolot S, Le GG, Scotet V, et al. HAMP as a modifier gene that increases the phenotypic expression of the HFE pC282Y homozygous genotype. *Blood.* 2004;103:2835-2840.
23. Biasiotto G, Belloli S, Ruggeri G, et al. Identification of new mutations of the HFE, hepcidin, and transferrin receptor 2 genes by denaturing HPLC analysis of individuals with biochemical indications of iron overload. *Clin Chem.* 2003;49:1981-1988.
24. Rivera S, Liu L, Nemeth E, et al. Hepcidin excess induces the sequestration of iron and exacerbates tumor-associated anemia. *Blood.* 2005;105:1797-1802.
25. Ganz T. Hepcidin: a regulator of intestinal iron absorption and iron recycling by macrophages. *Best Pract Res Clin Haematol.* 2005;18:171-182.
26. Hunter HN, Fulton DB, Ganz T, Vogel HJ. The solution structure of human hepcidin, a peptide hormone with antimicrobial activity that is involved in iron uptake and hereditary hemochromatosis. *J Biol Chem.* 2002;277:37597-37603.
27. Henikoff S, Henikoff JG. Amino acid substitution matrices from protein blocks. *Proc Natl Acad Sci U S A.* 1992;89:10915-10919.
28. Futami J, Tada H, Seno M, Ishikami S, Yamada H. Stabilization of human RNase 1 by introduction of a disulfide bond between residues 4 and 118. *J Biochem (Tokyo).* 2000;128:245-250.
29. Roetto A, Camaschella C. New insights into iron homeostasis through the study of non-HFE hereditary haemochromatosis. *Best Pract Res Clin Haematol.* 2005;18:235-250.
30. Biasiotto G, Daraio F, Cavallero G, et al. Homozygous or compound heterozygous R59G mutation of hepcidin gene in patients with adult-onset hemochromatosis [abstract]. *Bioiron 2005 Abstracts.* 2005;P139.
31. Fra AM, Fagioli C, Finazzi D, Sitia R, Alberini CM. Quality control of ER synthesized proteins: an exposed thiol group as a three-way switch mediating assembly, retention and degradation. *EMBO J.* 1993;12:4755-4761.
32. Schmiel A, Breitling F, Winter CH, Queitsch I, Dubel S. Effects of unpaired cysteines on yield, solubility and activity of different recombinant antibody constructs expressed in *E. coli*. *J Immunol Methods.* 2000;242:101-114.
33. Rivera S, Nemeth E, Gabayan V, et al. Synthetic hepcidin causes rapid dose-dependent hypoferrremia and is concentrated in ferroportin-containing organs. *Blood.* Prepublished on June 2, 2005, as DOI 10.1182/blood-2005-04-1766. (Now available as *Blood.* 2005;106:2196-2199).
34. Lin L, Goldberg YP, Ganz T. Competitive regulation of hepcidin mRNA by soluble and cell-associated hemojuvelin. *Blood.* Prepublished on July 5, 2005, as DOI 10.1182/blood-2005-05-1845. (Now available as *Blood.* 2005;106:2884-2889).